CHAPTER 21

A Parametric Model for Random Wave Deformation by Breaking on Arbitrary Beach Profiles

Hyuck–Min Kweon[1] and Yoshimi Goda[2]

Abstract

The process of wave energy dissipation after breaking has been investigated with a number of random wave tests. To obtain the data for wave breaking and its deformation, experiments have been conducted by utilizing a horizontal step adjoining to a combined slope of 1/20 and 1/10.

After breaking, the wave height decreases by dissipation but attains a certain value at some distance from the breaking point. Experimental results show that the stable wave height is not constant but affected considerably by the wave period. The study has yielded a general formulation of stable wave height due to the random wave breaking.

A new one-dimensional random wave deformation model is proposed, being coupled with nonlinear shoaling coefficient formula before wave breaking and the new energy dissipation term after breaking. The model is compared with the experimental data, large wave tank data, and field data. It predicts well the wave height deformation and the change of mean water level before and after wave breaking on arbitrary bottom profiles.

1 Introduction

Random wave breaking is one of the most important phenomena in coastal engineering. Since around 1970, various models have been proposed to predict wave height variations in the surf zone. Many models assume planar beach profiles. However, in the natural sea there are step type beach profiles, and longshore bars appear in the breaking zone. Thus, a workable model applicable to arbitrary beach profiles is needed.

The difference among existing models lies on how to express the dissipation

---

1) Researcher, TETRA Co., Ltd., 2-7 Higashi Nakanuki, Tsuchiura, Ibaraki, 300, Japan

2) Professor, Department of Civil Engineering, Yokohama National University, 79-5 Tokiwadai, Hodogaya-ku, Yokohama, 240 Japan

term. Takayama et el. (1991) proposed a model that calculates the dissipation term with a modified Rayleigh distribution. Battjes and Janssen (1978) represented it with a bore model. The concept of stable wave height after wave breaking was introduced by Dally et al. (1985). That is, after breaking, the wave height decreases by dissipation but attains a stable value at some distance from the breaking point. However, existing models have certain problems. Some models are applicable to plane beaches only, some requires clumsy computation for a joint probability density of wave heights and periods, and some others need calibration with individual wave data in the field.

The present study gives a formulation of the stable wave height due to the random wave breaking and aims at presenting a model simple enough but reasonably accurate.

2 Experiments

2-1 Experimental conditions

Tests were conducted in a glass walled tank of 17 m long, 0.5 m wide, and 0.55 m as shown in Fig. 1. A horizontal step of 6 m long was set, adjoining to the combined slopes of 1/10 with the length 2.0 m and 1/20 with the length 1.0 m. The motion of the wave generator was controlled to absorb waves reflected from slopes. The crushed stone slope of 13/100 was built at the end of horizontal step. Buoyant artificial material was also used as a dissipater together with the crushed stone. The height of horizontal step was 25 cm.

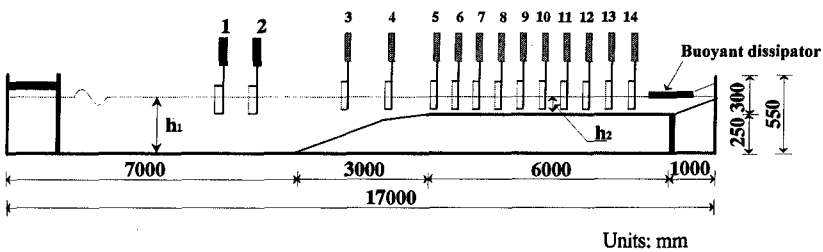

Fig. 1 Experimental section and measuring points for obtaining stable wave height

The wave profiles were recorded at 14 points. Measurements were made at 8 points simultaneously. Gauge #1 was fixed at the distance 3 m from the wave paddle and gauge #2 changed its location depending on the wave period for separation of incident and reflected waves utilizing the Goda and Suzuki (1976) method. Gauge #5 was set at the tip of horizontal step. On the horizontal step, 9 wave gauges from gauge #6 to #14 were set with the interval of 60 cm each.

Experiments are divided into two groups. One is for estimation of the bottom friction effect. The other is for obtaining fundamental data of wave height decay.

Firstly, nonbreaking waves were utilized for the estimation of wave attenuation due to bottom friction on a horizontal step. In total, 18 cases were tested with the water depth on the step of 9 cm and 11 cm, 3 types of spectrum, and 3 combinations of wave periods and heights.

Secondly, wave profiles were measured for obtaining the data of wave height decay by breaking and stable wave height. With 3 different shapes of spectrum, 2 water depths, 3 periods, and 3 wave heights, a total of 54 cases was tested. Wave heights were measured at 14 points as shown in Fig. 1. The sampling interval was 0.05 sec and 8192 data were collected at one run. Wave heights were determined from the surface elevation records using the zero down-crossing method.

2-2 Analysis of wave data

Investigation of wave spectra at gauges #1 or #2 indicated a presence of appreciable low frequency energy. However, there was a noticeable drop of spectral density between the main wave component and the low frequency components. The frequency of spectral density drop was indentified for each case, and the wave components lower than that frequency was filtered out. The filtered wave profiles were produced by the inverse FFT technique.

The frequency range for separating incident and reflected waves was from 0.6 to 3 times the peak frequency. The magnitude of wave attenuation in wave height due to friction was estimated with the data of nonbreaking waves. The wave profiles obtained from gauges #5 to #14 on the horizontal step were analyzed by the FFT method for the Fourier coefficients.

Iwagaki et al. (1965) derived the solution of wave attenuation by bottom friction based on the laminar flow theory. The solution was used to yield the following formula for wave amplitude correction.

$$a_{cor} = a_{mes} \exp\left(-C_{amp}\varepsilon_{b+w}\, x/L\right) \tag{1}$$

where

$$\varepsilon_{b+w} = \left(4\pi^2/\beta L\right)\left(1 + 1/\psi_0\right)\left(\sinh 2kd_0 + 2kd_0\right) \tag{2}$$

$$\beta = \left(\pi/\nu T\right)^{1/2} \tag{3}$$

$$\psi_0 = k\,B/\sinh 2kd_0 \tag{4}$$

in which a_{cor} is the amplitude of corrected Fourier coefficient, a_{mes} the amplitude of measuring data, C_{amp} ($\geq$1.0) an amplifier coefficient, x the distance from the initiation of horizontal step, L the wave length at a local point, T the wave period, k the wave number, d_0 the still water depth, ν the kinematic viscosity of water, and B the width of a water tank. The value of C_{amp} was estimated with nonbreaking waves corresponding to different shapes of spectrum. The results were 1.48 for the JONSWAP-type spectrum with γ=1.0, 1.74 for the spectrum with γ=3.3, and 2.19 for an extremely high concentrated spectrum with γ=10.0, respectively.

The decomposed Fourier amplitudes were corrected for the bottom friction

effect with eq. (1). Then, all the corrected amplitudes were utilized in the inverse FFT method to reproduce wave profiles. Wave heights were determined from the reproduced profiles.

3 Estimation of Stable Wave Heights after Random Wave Breaking

The stable height at some distance from the breaking point is proportional to the local water depth. In the experiments of Horikawa and Kuo (1966) the test bottom profile consisted of a steep slope section of 1 to 5 followed by a less steep slope (up to 1 to 20) or a horizontal section. The incident waves were forced to break at the end of the steep slope section and the wave height decay after breaking was monitored. It was fitted by exponential functions toward a stable wave height that is equal to about 0.4 times of the local water depth (d_0) for all conditions. The results of Horikawa and Kuo were interpreted by Dally et al. (1985) in terms of a wave height stabilizing at a constant value (cessation of breaking) lower than that related to the initiation of breaking.

The present study re-analyzed the Horikawa and Kuo (1966) data, by fitting the following exponential function:

$$H = H_0 \exp(-\varepsilon_{b+w} x/d_0) + H_s \tag{5}$$

where H_0 is the wave height at the initiation of the horizontal step. The stable wave height H_S was estimated with a bisection method.

All the stable wave heights were classified by water depth and wave period of 20 groups. Dally et al (1985) assumed that the stable height is proportional of water depth only. However, the height-to-depth ratio is not constant but affected considerably by the wave period as shown in Fig. 2 for the cases of regular waves. As shown in Fig. 2, the longer the wave period is, the higher the stable wave height is.

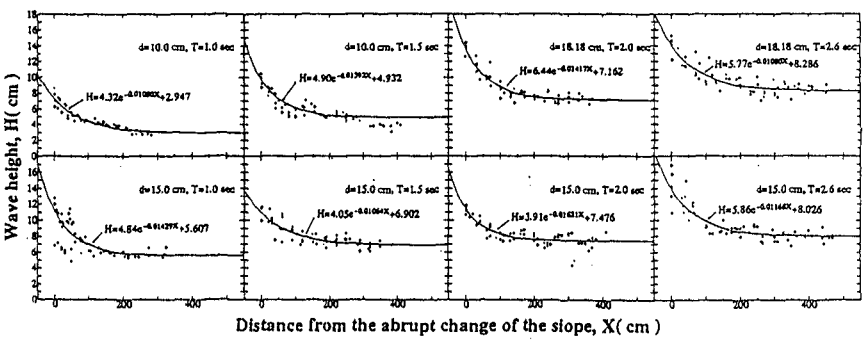

Fig. 2 The effect of wave period to a stable wave height

With the same procedure, the stable wave heights after random wave breaking

were estimated. In the random wave system, however, the stable wave heights have different levels corresponding to the definition of representative wave heights such $H_{1/3}$ and H_{rms}. The experimental results are plotted in Fig. 3.

Figure 3 indicates that the stable wave height is a function of the relative water depth d_0/L_0. For the experimental data, the following formulation has been applied in an analogy to Goda's breaker index:

$$H_s = \Gamma d \tag{6}$$

where

$$\Gamma = A(d_0/L_0)^{-1}\left[1-\exp(-1.5\pi d_0/L_0)\right] \tag{7}$$

$$d = d_0 + \overline{\eta} + \overline{\xi} \tag{8}$$

in which A is the coefficient for stable wave height. The symbol d_0 refers to the still water depth, L_0 the deep water wave length corresponding to the significant wave period, $\overline{\eta}$ the wave set-up, and $\overline{\xi}$ the representative amplitude of surf beat.

The curves in Fig. 3 represents the computation with eqs. (6) to (8).

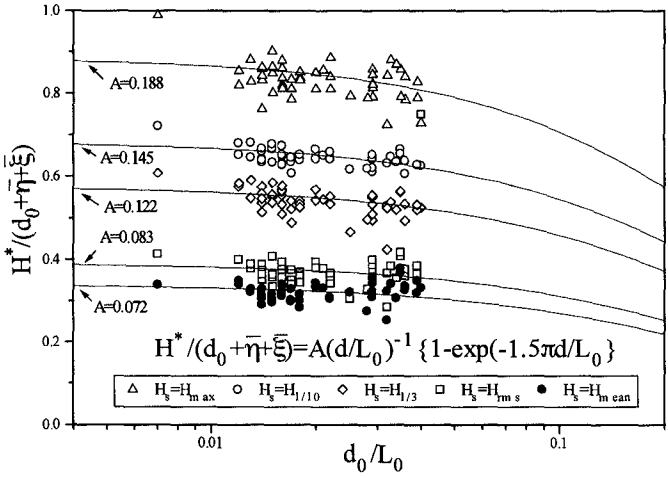

Fig. 3 The general form of stable wave heights due to breaking of random wave

The total water depth including the representative surf beat amplitude was assumed as below.

$$d_0 + \overline{\eta} + \overline{\xi} = d_0 + \chi\overline{\eta} \tag{9}$$

By assuming the value of χ at 1, 2, and 3, the least square method was applied for the relationship between the ratio of the significant wave height to the total depth and the relative water depth. It was found the linear fitting has the least value when χ is equal to 2. That means, it is best to set the representative surf beat amplitude $\overline{\xi}$ equal to the

wave set-up $\overline{\eta}$.

Table 1 lists the best fitted values of stable wave height coefficient A in eq. (7), for various representative wave heights.

Table 1 The stable wave height coefficients of A for various representative waves.

H	mean	*rms*	1/3	1/10	max
A	0.072	0.083	0.122	0.145	0.188

4 Modeling of Random Wave Deformation

4-1 Governing equation

Dally et al (1985) proposed a model to describe wave decay in the surf zone assuming that the energy dissipation per unit surface area due to breaking is proportional to the excess energy flux relative to a stable energy flux, which is depth dependent.

$$\frac{\partial EC_g}{\partial x} = \frac{-K_d}{d_0}\left[EC_g - \left(EC_g\right)_s\right] \tag{10}$$

where E is the energy density, C_g the group velocity, x the onshore coordinate, K_d the wave decay coefficient, and d_0 the still water depth. The energy density and group velocity are given by the linear theory relationships.

Rewriting eq. (10) in terms of wave height, it becomes as below:

$$\frac{\partial\left[H^2 C_g\right]}{\partial x} = -\frac{K_d}{d} C_g\left[H^2 - H_s^2\right] \tag{11}$$

where $H_s = \Gamma d$.

The present model adopts eq. (11) as the basis of computation and employs the stable wave height expressed by eq. (7). The wave decay coefficient K_d is specified with a gradually varying value, the treatment of which is discussed in detail in the next section.

The wave-induced set-up and set-down are determined from the time-averaged momentum balance equation neglecting inertial effects and bed-sheer stress, as follows :

$$\frac{d\overline{\eta}}{dx} = -\frac{1}{\rho g\left(d + \overline{\eta}\right)}\frac{dS_{xx}}{dx} \tag{12}$$

in which S_{xx} is the onshore radiation stress. The radiation stress component S_{xx} for the organized wave motion is calculated by the linear theory as

$$S_{xx} = \frac{1}{16}\rho g H_{rms}^2 \left[1 + \frac{4kd}{\sinh 2kd} \right] \tag{13}$$

where ρ is the density of water, g the acceleration due to gravity, k the wave number, and d the total water depth ($d = d_0 + \overline{\eta} + \overline{\xi}$).

4-2 Treatment of wave decay coefficient

The dissipation term with the wave decay coefficient K was originally proposed by Dally and Dean (1985) who gave a constant value. For the analysis of random wave deformation, however, a modification is made on the decay coefficient in such a way that its value gradually increases over some distance.

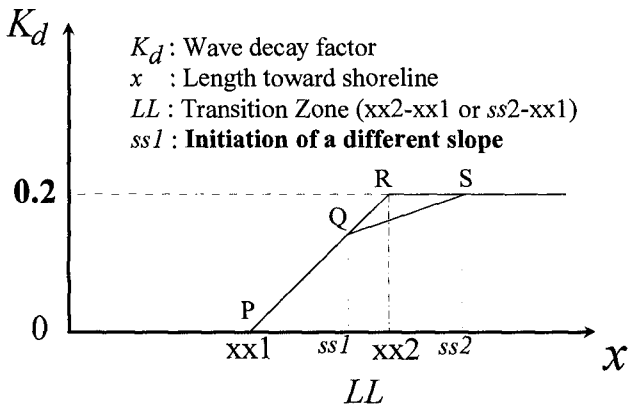

Fig. 4 Treatment of wave decay coefficient, K_d

The modification reflects the fact that waves have the different locations of initiation of breaking in a random wave system. Figure 4 shows the treatment of wave decay coefficient. For a single slope, K_d rises along the line PR over the locations between $xx1$ and $xx2$ and then takes a constant value of 0.2. The distance between $xx1$ and $xx2$ is calculated as the horizontal length corresponding to the change in water depth equivalent to the vertical distance of H_0'. If the slope becomes milder at the location $ss1$, then K_d follows the line QS. By introducing such a gradually varying wave decay coefficient, it becomes possible to calculate the wave decay successfully with the representative waves of a random wave system. It is also possible to analyze the wave deformation across beaches of arbitrary shapes.

The model has been calibrated with the Goda model (1975) for random wave breaking on a plane beach. The maximum value for the wave decay coefficient K_d and the transition length LL are calibrated to yield the best agreement between the present and Goda models. The comparison of the present and Goda model is shown in Fig. 5.

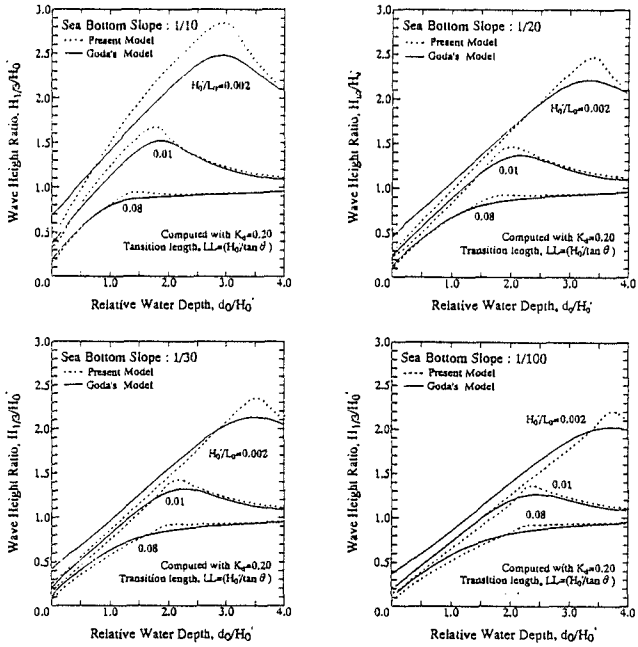

Fig. 5 Comparison of the present model with K_d=0.2 and the Goda model on plane beach

4-3 Procedure of calculation

Calculation is proceeded by a forward-difference numerical solution scheme from the offshore end of the numerical grid. The incident wave conditions of the model are the representative wave heights and the significant wave period. The non-linear wave shoaling is considered in the model.

Because eq. (11) produces a linear wave shoaling before wave breaking, the resultant wave height is amplified by the factor β of the following

$$\beta = K_s / K_{s0} \tag{14}$$

where

$$K_s = K_{s0} + 0.0015(d_0/L_0)^{-2.87}\left(H_0'/L_0\right)^{1.27} \tag{15}$$

in which K_s is a nonlinear shoaling coefficient, K_{s0} the linear shoaling coefficient, and H_0' the equivalent deep water significant wave height. The nonlinear shoaling coefficient of eq. (14) is obtained by the trial and error method as an approximation to Shuto's (1974) shoaling coefficient for non-breaking nonlinear wave based on cnoidal wave theory.

For initiation of wave breaking, Goda's breaking index of the following is adopted:

$$H_b = \Gamma_b d \tag{16}$$

where

$$\Gamma_b = A(d_0/L_0)^{-1}\left\{1-\exp\left[-1.5\frac{\pi d_0}{L_0}\left(1+15\tan^{4/3}\theta\right)\right]\right\} \tag{17}$$

in which H_b refers to the respective breaker heights of representative waves such as $H_{1/3}$ and A is the coefficient listed in Table. 1.

After wave breaking is initiated, the wave decay coefficient K_d in eq. (11) is assigned the value which rises up following the path PR or PQS and the energy dissipation is evaluated. For the calculation of nonlinear wave decay height, the stable wave height is modified as

$$(H_s)_A = \frac{1}{1+\beta_b}(H_s)_F \tag{18}$$

where $(H_s)_A$ is the linear stable wave height, $(H_s)_F$ the non-linear stable wave height which was attained by experiments as in eq. (6), and β_b is the amplification factor of shoaling coefficient ratio at the initiation point of breaking.

After wave breaking has occurred, a check is always made for the possibility of wave reformation. That is, if the calculated wave height falls below the stable wave height even though the K_d does not attain the maximum value of 0.2, K_d is reset as zero at that point. Then calculation starts again in the process of shoaling change.

Calculation of radiation stress by eq. (13) is needed before that of wave set-up by eq. (12). The root-mean-square wave height is calculated from $H_{1/3}$ with the assumption of Rayleigh distribution.

$$H_{rms} = H_{1/3}/1.416 \tag{19}$$

The computation of wave height and set-up is carried out twice. In the first run, the wave set-up at the shoreline where the still water depth is zero is linearly extrapolated from the adjacent two grid points. In the second run, the wave set-up and representative surf beat amplitude are added to the still water depth to yield the total depth. The present model finishes the calculation for all points at the second run because the difference of wave set-up between the 2nd and 3rd runs becomes below 2%.

5 Verification of the Model

5-1 Laboratory tests on a horizontal step adjoining to slope

Figure 6 shows the comparison of the model calculation and experimental data obtained from the present study. The increment of x in the calculation is 5 cm. The data with the JONSWAP-type spectrum (γ=3.3) are selected for comparison. Three

sets of data in which the wave steepness is almost the same but the water depth is different are shown here. As seen in Fig. 6, even when the water depth is extremely shallow, the model predicts the wave decay height quite well.

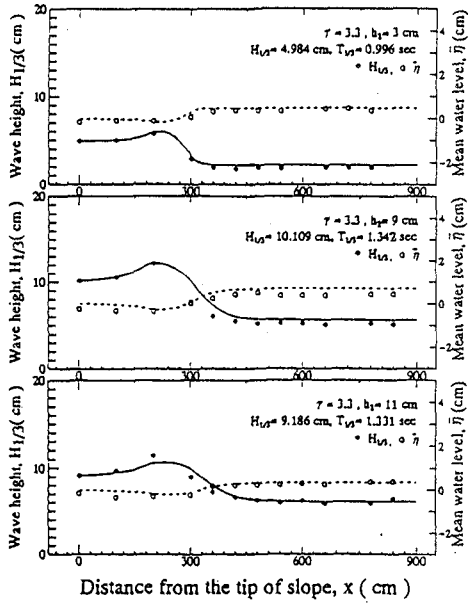

Fig. 6 Comparison of the model and experimental data on a horizontal step adjoining to slopes

5-2 Laboratory tests on a bar type beach profile

For obtaining data in a bar type beach profile, experiments were conducted with the section shown in Fig. 7. The wave profiles were measured at 14 points. Waves were expected to break between gauges #3 to #5 and to attain stable wave height between gauges #9 to #11. After waves become stable, waves start a shoaling change and re-break around gauges #12 to #13. Gauges #4 to #13 were set with the interval of 50 cm. The distance between gauges #13 and #14 was changed depending on wave period from 50 cm to less than 50 cm. The wave conditions included 3 diffe-

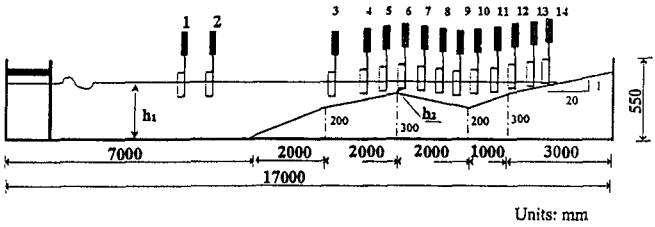

Fig. 7 Experimental setup for bar type beach profile

rent shapes of spectrum, 2 water depths, 3 wave periods, and 3 wave heights, and 54 cases were tested totally. The water depth in front of the wave paddle was h_1=39 cm and the depth on top bar was h_2=9 cm.

A selected set of experimental data with the JONSWAP-type spectrum (γ=1.0) is compared with the model calculation in Fig. 8. As shown in Fig. 8, the significant wave height (closed circles) shows good agreement except for the case with the largest wave steepness (top figure). However, the root-mean-square wave height (closed triangle) is predicted well by the model. During the wave decay height, it arrives a stable wave and increase with shoaling change. And it breaks again and decays toward the shoreline

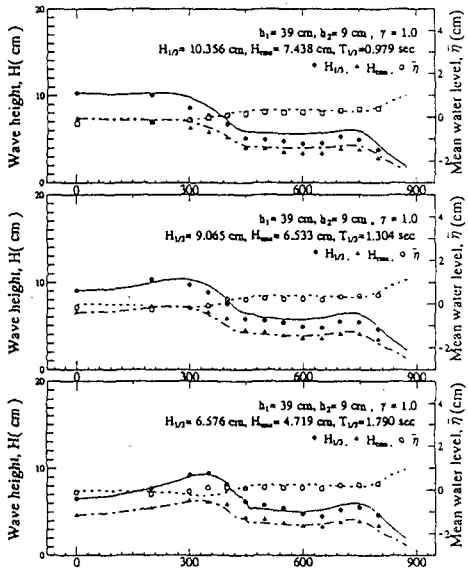

Fig. 8 Comparison of the model and data on a bar type profile

Moreover, variation of wave set-up (open boxes) is predicted quite well by the present model. Though not presented in this paper, experimental data with other spectral shapes have also shown good agreement with the calculation by the present model. Thus, the model is applicable broadly to different shapes of spectrum.

5-3 SUPERTANK data

Four cases from the SUPERTANK Data Collection Project (Kraus et al. 1992) were selected to validate the random wave deformation model for normally incident waves under controlled conditions. SUPERTANK was conducted to investigate cross-shore hydrodynamic and sediment transport process using the large wave tank at Oregon State University, Corvallis, Oregon. In this study, the statistical data are utilized and no spectral information is used.

In the case A0517A, a pronounced bar was present with the crest located at a water depth of about 0.6 m. Case A0914A belongs to the same run as the previous case, but the bar was located further offshore. In the case S0913A a narrow-crested mound was constructed. A broad-crested mound was built in the offshore in the case S1208B.

Table 2 Wave conditions for compared SUPERTANK data

Run Number	Case number	Incident wave height		Wave period
		rms (m)	$H_{1/3}$ (m)	(sec)
ST10	A0517A	0.56	0.79	2.9
ST10	A0914A	0.51	0.71	3.8
STJ0	S0913A	0.45	0.63	2.8
STK0	S1208B	0.45	0.64	2.7

The data of $H_{1/3}$, H_{rms} and $\overline{\eta}$ are plotted in Fig. 9 with the symbols of closed boxes, closed circles, and open circles, respectively. The computed results are shown by the dash-dot lines, continuous lines, and dashed lines, respectively.

In the case A0517A, the wave breaking by computing starts prior to the data. The significant wave height is predicted well by the model. Case A0914A belongs to the same run as previous case but has longer wave period. The decay in H_{rms} and $H_{1/3}$ through the surf zone are well produced. However, it seems that the wave height nearest to the bar is affected by concentrating of wave breaking. The starting of set-up is affected by the initiation of breaking points.

In the case S0913A, the decays in H_{rms} and $H_{1/3}$ are faithfully produced by the model. However, the wave set-up is lower than the computation. In the case S1208B which has the broader bar, the model overestimates the wave heights around crest of the bar. It seems that on the crest the waves are not strongly affected by the wave nonlinearity.

5-4 Field data

Hotta and Mizuguchi (1980) carried out field measurements in 1978 at Ajigaura beach facing the Pacific Ocean located at the southern end of Tokai coast about 200 km from Tokyo. A breaker bar was present in the surf zone as shown in Fig. 10. In the nearshore zone, about sixty poles were placed on the sea bed at intervals of about 2 m normal to the shore over a total distance of 120 m. The significant wave at the latter pole was about 0.8 m in height and 9.4 sec in period.

Figure 10 shows the measured and computed wave heights. The computed wave heights before breaking are greater than the measured ones. The measured wave heights do not increase much in the zone between 120 to 100 m. The reason is not quite clear. It may be related to the bathymetry of the field. Dally and Dean(1986) also made comparison of their model and the data. Their prediction shows underestimation of the data because they used the linear shoaling.

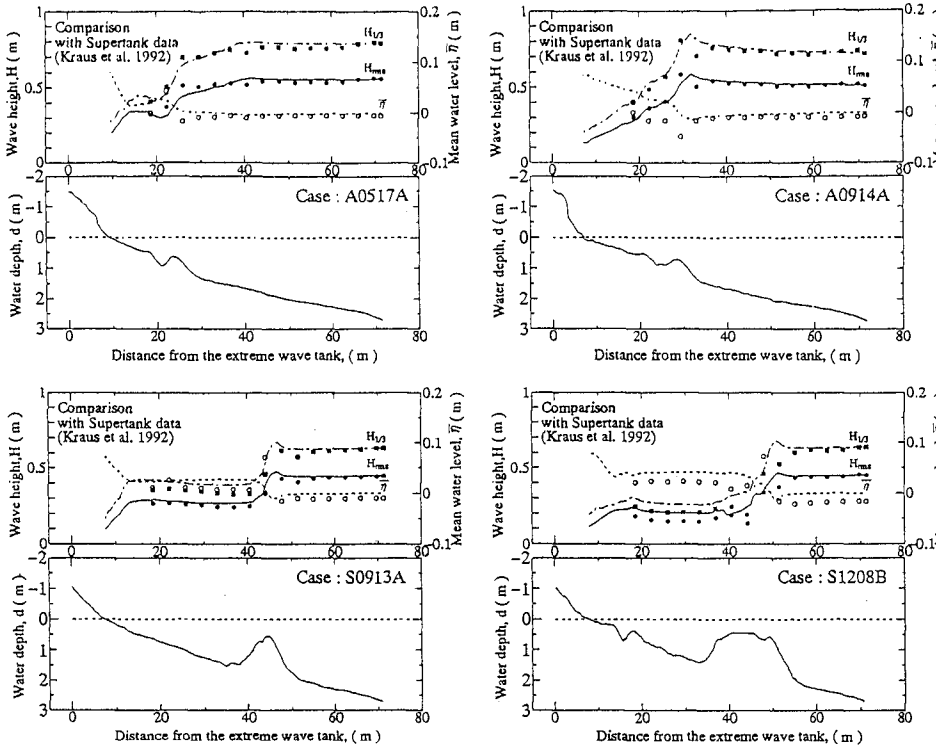

Fig. 9 Comparison of the model and SUPERTANK data

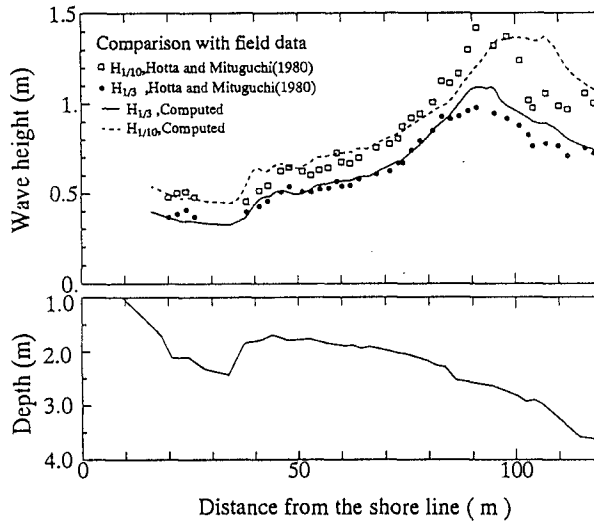

Fig. 10 Comparison of the model and field data

6 Conclusion

The merits of the present model are summarized as follows:

1) The model is applicable to any shapes of bottom profiles.
2) It requires the input data of incident wave heights and periods only without necessity of coefficient calibration with field data.
3) Its computation time is minimal because it deals with representative waves directly.

In addition, the model can easily be programmed as a subroutine for a large scheme to drive numerical models of nearshore circulation and sediment transport problems.

Acknowledgment

The authors would like to thanks Dr. Kraus, Dr. Smith and all the members who participated the SUPERTANK project. They offered valuable data for verification of the present model.

References

Battjes, J. A. and J.P.F.M. Janssen, 1978. Energy loss and setup due to breaking of random waves. Proc. 16th Coast. Eng. Conf., pp.567-587.

Dally, W.R., 1992. Random breaking waves : field verification of a wave-by-wave algorithm for engineering application, Coastal Eng., Vol. 16, pp. 369-397.

Dally, W.R. and R.G Dean, 1986. Transformation of random breaking waves on surf beat. Proc. 20th Coast. Eng. Conf., Vol. 1, pp. 109-123.

Dally, W.R., R.G. Dean, and R.A. Dalrymple, 1985. Wave height variation across beaches of arbitrary profiles, J. Gephys. Res., 90(C6), pp. 11917-11927.

Goda, Y., 1975. Irregular wave deformation in the surf zone. Coast. Eng. Jpn, Vol. 18, pp. 12-26.

Mase, H. and Y. Iwagaki, 1982. Wave height distribution and wave grouping in surf zone. Proc. 18th Coast. Eng. Conf., pp. 58-76.

Horikawa, K and C.T. Kuo, 1966. A study on wave transformation inside surf zone. Proc. 16th Coast. Eng. Conf., Vol. 1, pp. 217-233.

Hotta, S. and M. Mizuguchi, 1980. A field study of waves in the surf zone. Coastal Eng. Jpn., Vol. 23, pp. 59-81.

Iwagaki, Y. and Y. Tsuchiya, 1966. Laminar damping of oscillatory waves due to bottom friction. Proc. 10th Coast. Eng. Conf., pp. 149-174.

Kraus, N. C., J. M. Smith, and C. K. Sollitt, 1992. SUPERTANK laboratory data collection project. Proc., 23th Coast. Eng. Conf., pp. 2191-2204.

Larson, M., 1995. Model for decay of random waves in surf zone. J. Wtrwy., Port, Coast., Oc., Engrg., ASCE, pp. 1-12.

Shuto, N., 1974. Non-linear long waves in a channel of variable section. Coastal Eng. Jpn., Vol. 17, pp. 1-12.